

MIT Open Access Articles

Improved Measurement of the Rossiter-McLaughlin Effect in the Exoplanetary System HD 17156

The MIT Faculty has made this article openly available. **Please share** how this access benefits you. Your story matters.

Citation: Narita, Norio et al. "Improved Measurement of the Rossiter-McLaughlin Effect in the Exoplanetary System HD 17156." Publications of the Astronomical Society of Japan 61 (2009): 991-997.

As Published: <http://arxiv.org/abs/0905.4727>

Publisher: Astronomical Society of Japan

Persistent URL: <http://hdl.handle.net/1721.1/76743>

Version: Author's final manuscript: final author's manuscript post peer review, without publisher's formatting or copy editing

Terms of use: Creative Commons Attribution-Noncommercial-Share Alike 3.0



Improved Measurement of the Rossiter-McLaughlin Effect in the Exoplanetary System HD 17156*

Norio NARITA,¹ Teruyuki HIRANO,² Bun'ei SATO,³ Joshua N. WINN,⁴ Yasushi SUTO,²
Edwin L. TURNER,^{5,6} Wako AOKI,¹ Motohide TAMURA,¹ and Toru YAMADA⁷

¹ *National Astronomical Observatory of Japan, 2-21-1 Osawa, Mitaka, Tokyo, 181-8588, Japan*
norio.narita@nao.ac.jp

² *Department of Physics, The University of Tokyo, Tokyo, 113-0033, Japan*

³ *Global Edge Institute, Tokyo Institute of Technology, 2-12-1 Ookayama, Meguro, Tokyo, 152-8550, Japan*

⁴ *Department of Physics, and Kavli Institute for Astrophysics and Space Research, Massachusetts Institute of Technology, Cambridge, MA 02139, USA*

⁵ *Princeton University Observatory, Peyton Hall, Princeton, NJ 08544, USA*

⁶ *Institute for the Physics and Mathematics of the Universe, The University of Tokyo, Kashiwa, 277-8568, Japan*

⁷ *Astronomical Institute, Tohoku University, Aramaki, Aoba, Sendai, 980-8578, Japan*

(Received 2009 April 27; accepted 2009 May 28)

Abstract

We present an improved measurement of the Rossiter-McLaughlin effect for the exoplanetary system HD 17156, based on radial-velocity data gathered with the Subaru 8.2m telescope throughout the planetary transit of UT 2008 November 7. The data allow for a precise and independent determination of the projected spin-orbit angle of this system: $\lambda = 10.0^\circ \pm 5.1^\circ$. This result supersedes the previous claim of $\lambda = 62^\circ \pm 25^\circ$ by Narita et al., which was based on lower-precision data with poor statistics. Thus the stellar spin and planetary orbital axes of the HD 17156 system are likely to be well-aligned, despite the planet's large orbital eccentricity suggesting a history of strong dynamical interactions.

Key words: stars: planetary systems: individual (HD 17156) — stars: rotation — techniques: photometric — techniques: radial velocities — techniques: spectroscopic

* Based on data collected at Subaru Telescope, which is operated by the National Astronomical Observatory of Japan.

1. Introduction

The discoveries of more than 340 extrasolar planets have revealed the remarkable diversity of planetary systems. For example, many Jovian planets lie far inside the snow line, and many of their orbits are more eccentric than the orbits in the Solar system. This diversity of planetary systems has prompted theorists to consider new modes of planet formation and migration, including Type II migration models (e.g., Lin & Papaloizou 1985; Lin et al. 1996; Ida & Lin 2004), planet-planet scattering models (e.g., Rasio & Ford 1996; Marzari & Weidenschilling 2002; Nagasawa et al. 2008; Chatterjee et al. 2008), and Kozai cycles (with tidal friction) for planets in binary systems (e.g., Wu & Murray 2003; Takeda & Rasio 2005; Fabrycky & Tremaine 2007; Wu et al. 2007). In particular, planet-planet scattering and the Kozai effect may help to explain the eccentric orbits of close-in planets, since Type II migration alone does not seem to produce large orbital eccentricities.

Observations of transiting planets may lead to better understanding of migration mechanisms through the Rossiter-McLaughlin effect (hereafter the RM effect: Rossiter 1924, McLaughlin 1924). The RM effect is an apparent radial-velocity anomaly that is observed during planetary transits (see Ohta et al. 2005; Giménez 2006; Gaudi & Winn 2007 for theoretical discussions). By measuring and modeling this anomaly, one can learn the sky-projected angle between the stellar spin axis and the planetary orbital axis, denoted by λ . The angle between these two axes has been recognized as an useful diagnostic to investigate planet migration histories. The basic premises are that planets are formed with their orbital axes parallel to the stellar rotation axis, that Type II migration maintains a small spin-orbit alignment angle, while planet-planet scattering and the Kozai effect may produce large spin-orbit misalignments (e.g., Nagasawa et al. 2008; Chatterjee et al. 2008), and that tidal effects do not subsequently alter the spin-orbit angle (Barker & Ogilvie 2009). To the extent that these premises are valid, observations of the RM effect in transiting planets allow us to test planet migration models. One may compare the distribution of observed spin-orbit alignment angles with theoretical predictions based on the scenarios of planet-planet scattering or Kozai cycles with tidal friction (Fabrycky & Winn 2009).

Measurement of the RM effect is especially interesting for transiting planets in eccentric orbits (hereafter “transiting eccentric planets” or TEPs), because the migration mechanisms that produce eccentric orbits may also produce large spin-orbit misalignments. The number of known TEPs is still small. Observations of the RM effect have been reported for a few cases, including HAT-P-2b (Winn et al. 2007b; Loeillet et al. 2008), XO-3b (Hébrard et al. 2008; Winn et al. 2009b), and the subject of this paper, HD 17156b.

HD 17156b was discovered in a Doppler survey (Fischer et al. 2007; F07) and later found to transit its parent star (Barbieri et al. 2007). This planetary system stands out among the transiting planets for its large orbital eccentricity ($e = 0.68$) and relatively long orbital

period (21 days). The host star is very bright ($V = 8.2$), facilitating the detection of the RM effect and many other follow-up observations. For the HD 17156 planetary system, previously Narita et al. (2008; N08) reported a possible spin-orbit misalignment $\lambda = 62^\circ \pm 25^\circ$, based on radial-velocity data obtained at the Okayama Astrophysical Observatory (OAO). A more decisive conclusion, however, required further precise observations with better statistics. Indeed Cochran et al. (2008; C08) and Barbieri et al. (2008; B08) obtained new radial-velocity data (C08: HET and HJST datasets, B08: TNG dataset), and claimed a close alignment, $\lambda = 9.4^\circ \pm 9.3^\circ$ (C08) and $\lambda = -4.8^\circ \pm 5.3^\circ$ (B08)¹.

We report here on our new observations with the Subaru 8.2m telescope, covering a full transit of HD 17156b and providing the larger and more precise radial-velocity dataset for the system around the transit phase. Section 2 summarizes our Subaru spectroscopic observations and radial-velocity dataset, and section 3 describes the analysis procedure for the RM effect. Section 4 presents and discusses the results for the derived system parameters. Section 5 summarizes the main findings of the present paper.

2. Subaru Spectroscopy and Radial Velocities

We observed HD 17156 over 6.5 hr covering a full transit of HD 17156b with the High Dispersion Spectrograph (HDS; Noguchi et al. 2002) on the Subaru 8.2m telescope on UT 2008 November 7. We employed the standard I2a set-up of the HDS, covering the wavelength range $4940 \text{ \AA} < \lambda < 6180 \text{ \AA}$ and using the Iodine gas absorption cell for precise radial velocity measurements. The slit width of $0''.4$ yielded a spectral resolution of ~ 90000 , and the seeing on that night was between $0''.4$ and $0''.7$. The exposure time was 3–5 minutes, yielding a typical signal-to-noise ratio (SNR) of approximately 180 per pixel. We processed the observed frames with standard IRAF² procedures and extracted one-dimensional spectra. We computed relative radial velocities following the algorithm of Butler et al. (1996) and Sato et al. (2002), as described in Narita et al. (2007). We estimated the internal error of each radial velocity as the scatter in the radial-velocity solutions among the $\sim 4 \text{ \AA}$ segments of the spectrum. The typical internal error is 3 m s^{-1} . The radial velocities and their internal errors are plotted in Figure 1 and summarized in Table 1.

3. Analysis Procedure

We empirically model the RM effect of HD17156 following the procedure of Winn et al. (2005). Specifically, we simulate spectra that are affected by the RM effect, and

¹ Note that B08 used $\beta(\equiv -\lambda)$ defined in Giménez (2006) for the projected spin-orbit alignment angle.

² The Image Reduction and Analysis Facility (IRAF) is distributed by the U.S. National Optical Astronomy Observatories, which are operated by the Association of Universities for Research in Astronomy, Inc., under cooperative agreement with the National Science Foundation.

then we “measure” the anomalous radial velocity of the simulated spectrum using the same algorithm that we use on the actual data. We start with the NSO solar spectrum (Kurucz et al. 1984) and deconvolve it to remove the rotational broadening of the Sun. We neglect the differential rotation of the Sun and adopt 1.85 km s^{-1} (the rotational velocity at the equator) for the deconvolution kernel. We then apply a rotational broadening kernel with $V \sin I_s = 2.6 \text{ km s}^{-1}$ as appropriate to mimic the disk-integrated spectrum of HD 17156 (F07). In this step, for simplicity, we neglect differential rotation, microturbulence and macroturbulence, convection cells, and possible starspots and other active regions. Finally, to simulate the RM effect, we subtract a scaled and velocity-shifted copy of the original unbroadened spectrum, representing the portion of the stellar disk hidden by the planet. We produce many simulated spectra using different values of the scaling factor f and the velocity shift v_p , and compute the apparent radial velocity of each spectrum. We thereby determine an empirical relation between the size of the planet and its position on the stellar disk, and the apparent radial velocity of the star. We fit a polynomial function to this relation, and find

$$\Delta v = -f v_p \left[1.314 - 0.304 \left(\frac{v_p}{V \sin I_s} \right)^2 \right]. \quad (1)$$

As has been found previously (e.g., Winn et al. 2005), this formula differs from the analytic formula presented by Ohta et al. (2005). The two formulas are nearly consistent, however, if we rescale the value of $V \sin I_s$ in the analytic OTS formula by a factor of 1.2. In this sense the OTS formula may overestimate the projected stellar rotational velocity by $\sim 20\%$. Further discussions for the empirical fitting formulae for the RM effect are presented in section 4.3.

We analyze the RM effect of HD 17156b using our new Subaru dataset, accompanied by published out-of-transit radial velocity datasets presented in F07 (Subaru) and Winn et al. (2009a; W09) (Keck). (The Keck dataset was originally taken by F07, and W09 refined the radial velocities and added new data.) The out-of-transit data are needed to determine the Keplerian orbital parameters of HD 17156b. After performing this analysis of the new transit data, we also repeated the analysis using all of the published radial-velocity datasets around the transit phase (N08, C08, and B08) for comparison. In all of our analyses we consider the error in each radial velocity data point to be the quadrature sum of the internal error and 3 m s^{-1} (representing possible systematic error such as “stellar jitter”).

For radial velocity fitting, we fix stellar and planetary parameters based on Barbieri et al. (2008) as follows; the stellar mass $M_s = 1.24 [M_\odot]$, the stellar radius $R_s = 1.44 [R_\odot]$, the radius ratio $R_p/R_s = 0.0727$, and the semi-major axis $a = 0.1614 [\text{AU}]$. We also fix the quadratic limb-darkening parameters for the spectroscopic band containing many Iodine absorption lines to $u_1 = 0.39$ and $u_2 = 0.37$ based on the tables of Claret (2004). In addition, we adopt an updated transit ephemeris based on simultaneous transit photometry as $T_c = 2454777.94761 [\text{HJD}]$ and $P = 21.2165298$ days based on unpublished data from the Transit Light Curve project (see e.g. Holman et al. 2006, Winn et al. 2007). The adopted parameters are summarized in Table 2.

Our model has 6 free parameters describing the HD 17156 system: the radial velocity semiamplitude K , the eccentricity e , the argument of periastron ω , the orbital inclination i , the sky-projected stellar rotational velocity $V \sin I_s$, and the sky-projected angle between the stellar spin axis and the planetary orbital axis λ . Our model also has one free parameter, a velocity offset, for each independent radial velocity dataset (v_1 : our Subaru dataset, v_2 : Subaru in F07, v_3 : Keck in W09, v_4 : HET in C08, v_5 : HJST in C08, v_6 : OAO in N08, v_7 : TNG in B08).

We calculate the χ^2 statistic

$$\chi^2 = \sum_i \left[\frac{v_{i,\text{obs}} - v_{i,\text{calc}}}{\sigma_i} \right]^2, \quad (2)$$

where $v_{i,\text{obs}}$ are the observed radial velocity data and $v_{i,\text{calc}}$ are the values calculated based on a Keplerian orbit and on the RM calibration formula given above. We determine optimal orbital parameters by minimizing the χ^2 statistic using the AMOEBA algorithm (Press et al. 1992), and estimate confidence levels based on the criterion $\Delta\chi^2 = 1.0$ when a parameter is stepped away from its optimal value and the other parameters are re-optimized.

4. Results and Discussions

4.1. Results for the Key Parameter λ

We first fit our Subaru dataset with the out-of-transit Subaru (F07) and Keck (W09) datasets. Figure 2 shows our Subaru dataset plotted with the best-fitting model curve. We find $\lambda = 10.0^\circ \pm 5.1^\circ$, indicating a fairly good alignment between the sky projections of the stellar spin axis and the planetary orbital axis. This value is similar to the result quoted by C08 ($\lambda = 9.4^\circ \pm 9.3^\circ$), which was based on F07, N08, and C08 datasets.

Next we conduct another analysis using all of the published datasets (namely, with F07, N08, C08, B08, and W09 datasets). Figure 3 plots all radial velocity data with the best-fitting model curve. In this case we find $\lambda = 0.8^\circ \pm 4.3^\circ$, and the results for the other parameters are in agreement with the previous analysis. The results of both analyses are summarized in Table 3. We note that the central value of λ for the combined analysis is somewhat biased by the TNG dataset. This is because the contribution to χ^2 from the TNG dataset is disproportionate ($\Delta\chi^2 = 55.73$ from 28 TNG radial velocities), whereas the ratio of $\Delta\chi^2$ contribution and the number of data points is approximately unity for all of the other datasets. This suggests that the errors in the TNG dataset may have been underestimated. For this reason the results of the joint analysis should be interpreted with caution.

In addition, we conduct the same fitting procedure for the OAO dataset; for the HET, HJST, and OAO datasets; and for the TNG dataset alone, in order to make comparisons with previous studies (N08, C08, and B08). Note that we employ the same assumptions as described in section 3, and we incorporate the out-of-transit velocities from the F07/Subaru

and W09/Keck datasets. The results are $\lambda = 57^\circ \pm 23^\circ$ (as compared to $\lambda = 62^\circ \pm 25^\circ$ by N08) for the OAO dataset; $\lambda = 11.0^\circ \pm 11.8^\circ$ ($\lambda = 9.4^\circ \pm 9.3^\circ$ by C08) for HET, HJST, and OAO datasets; and $\lambda = -33.7^\circ \pm 9.7^\circ$ ($\lambda = -4.8^\circ \pm 5.3^\circ$ by B08) for the TNG dataset. Consequently, we confirm that the OAO dataset indeed implies a large spin-orbit misalignment, but its poorer radial velocity accuracy and time-resolution would have caused the fluke with lower statistical significance. In addition, although our analyses are well consistent with N08 and C08, we are not able to reproduce the B08 result. The systematic difference may be caused by the fact that B08 first fitted only the out-of-transit data and determined a radial velocity offset (namely, the baseline of the Keplerian motion) of the TNG dataset using fewer samples than we have here. Such a treatment might be problematic since the RM amplitude of HD 17156b is only $\sim 15 \text{ m s}^{-1}$, and a difference of offset velocity as much as several m s^{-1} would cause a large systematic difference in λ .

4.2. Assessments of Some Systematic Errors

In the above analyses, we fixed some parameters as summarized in Table 2, which were independently determined by previous high accuracy photometric and spectroscopic studies. In order to check the robustness of our results and to estimate the level of systematic errors, we retry the fitting for our Subaru dataset, the F07 Subaru dataset, and the W09 Keck dataset with different adopted parameter values as follows; $u_1 = 0.59$ (a greater limb-darkening case); $u_1 = 0.19$ (a smaller limb-darkening case); $a/R_s = 21.1$ (1σ lower limit in W09); and $a/R_s = 25.0$ (1σ upper limit in W09). We note that we find R_p/R_s within its error reported in B08 and W09 does not make a significant difference in results (only $V \sin I_s$ is affected, and only by a few percent).

We first find that K , e , ω , and offset velocities are insensitive to the fixed parameters. In addition, respective results for the spin-orbit alignment angle λ are $10.8^\circ \pm 5.6^\circ$ ($u_1 = 0.59$); $9.9^\circ \pm 5.0^\circ$ ($u_1 = 0.19$); $5.8^\circ \pm 2.9^\circ$ ($a/R_s = 21.1$); and $13.4^\circ \pm 7.0^\circ$ ($a/R_s = 25.0$). Consequently, we confirm all results of λ for the test cases are well within our 1σ uncertainty.

In contrast, we find appreciable systematic errors in the inclination i and $V \sin I_s$. Results for the inclination i are $87.52^\circ \pm 0.36^\circ$ ($u_1 = 0.59$); $86.99^\circ \pm 0.31^\circ$ ($u_1 = 0.19$); $85.11^\circ \pm 0.21^\circ$ ($a/R_s = 21.1$); and $87.95^\circ \pm 0.40^\circ$ ($a/R_s = 25.0$). We thus conclude that the dependence of the inclination on the limb-darkening parameters is small (within $\sim 1\sigma$ error), but the dependence on a/R_s is as large as a few degrees (over 3σ). When the covariance with the a/R_s parameter is taken into account, our constraint on i based on the RM anomaly is approximately 84.90° – 88.35° . This is in good agreement with the constraint by W09 (85.4° – 88.3°). On the other hand, we derive the projected velocity of stellar rotation $V \sin I_s$ as, $4.08 \pm 0.32 \text{ km s}^{-1}$ ($u_1 = 0.59$); $4.18 \pm 0.31 \text{ km s}^{-1}$ ($u_1 = 0.19$); $5.08 \pm 0.41 \text{ km s}^{-1}$ ($a/R_s = 21.1$); and $4.02 \pm 0.30 \text{ km s}^{-1}$ ($a/R_s = 25.0$). Based on these results we find that the result for $V \sin I_s$ is more robust than that for i , but the true error is approximately 1 km s^{-1} (the span of the results just quoted).

We also consider possible time-correlated errors in the radial velocity datasets, due to possible instrumental or astrophysical effects. When present, this so-called “red noise” complicates the accurate estimation of parameter errors (Pont et al. 2006). To check for red noise in the Subaru dataset, we calculate the standard deviation of the residuals between the data and the best-fitting model, and also the time-averaged (binned) residuals. In the absence of time-correlated noise, the standard deviation of n -point binned residuals (σ_n) would decrease as

$$\sigma_n = \sigma_1 \left(\frac{1}{n} \frac{m}{m-1} \right)^{1/2}, \quad (3)$$

where m is the number of binned residuals. We find the standard deviation of residuals to be $\sigma_1 = 3.42 \text{ m s}^{-1}$, and if there is no correlated noise then we expect the standard deviation of 5-point binned residuals to be $\sigma_{5,\text{exp}} = 1.58 \text{ m s}^{-1}$. The actual standard deviation of residuals with 5-point binning is $\sigma_{5,\text{act}} = 1.69 \text{ m s}^{-1}$. This is only 7% larger than the expected value; apparently the level of time-correlated noise is small.

4.3. Notes on the RM Formulae

Winn et al. (2005) pointed out a systematic difference in the amplitude of the RM anomaly between the results of RM simulations and the analytic OTS formula for the HD 209458 system. A preliminary analysis of Hirano et al. (in prep.) indicates the systematic difference between the OTS formula and the RM simulations is due to the fact that the former computes the spectral shift via intensity-weighted average while the latter via the cross-correlation. Specifically, they showed that the amplitude of the systematics depends on the spin rotation velocity of the host star. Following their procedure, we also confirmed the similar systematics for the HD 17156 system using the Subaru analysis routine (section 3). In addition to that, we show in this subsection that the input value of the spin rotation velocity, more specifically $V \sin I_s$, in the empirical RM formula does not bias the estimate of the other parameters.

When we fit our Subaru dataset using the OTS formula, we find $V \sin I_s = 5.03 \text{ km s}^{-1}$, which is $\sim 20\%$ higher than the result using the simulation-based formula. The results for all the other parameters are essentially unchanged. Thus the choice of the RM calibration formula corresponds to a $\sim 20\%$ change in the inferred value of $V \sin I_s$. We also expect that the formula of Giménez (2006) would give similar results to the OTS formula, as both formulas were calculated under the same assumption: that the anomalous radial velocity is equal to the shift in the intensity-weighted mean wavelength of the absorption lines.

In the previous studies, the $V \sin I_s$ value assumed for the simulation was generally in agreement with the resultant fitted value. However, we obtained $V \sin I_s = 4.18 \pm 0.31 \text{ km s}^{-1}$ from the RM analyses even though we assumed $V \sin I_s = 2.6 \text{ km s}^{-1}$ in the simulations. Ideally the fitted value of $V \sin I_s$ should be consistent with the assumed one. In order to check the dependence of assumed $V \sin I_s$ value on fitting results, we reran the simulations assuming $V \sin I_s = 4.2 \text{ km s}^{-1}$ for the convolution kernel instead of the original choice of 2.6 km s^{-1} . The

revised empirical formula is

$$\Delta v = -f v_p \left[1.367 - 0.505 \left(\frac{v_p}{V \sin I_s} \right)^2 \right]. \quad (4)$$

With this revised formula, we repeated the analysis using the Subaru dataset along with the F07 and W09 datasets. We find $V \sin I_s = 4.22 \pm 0.31 \text{ km s}^{-1}$ and the values of the other parameters are essentially unchanged. The results are now self-consistent and suggest that the choice of an empirical formula does not make a significant difference. Thus we conclude that the determination of λ of the current system is fairly insensitive to the choice of the RM formula.

5. Summary

We observed a full transit of HD 17156b with the Subaru 8.2m telescope, and measured radial velocities with the highest time-resolution and accuracy that have yet been presented for transit observations of this system. We analyzed the RM effect and found that the sky-projected spin-orbit alignment angle of the HD 17156 system is $\lambda = 10.0^\circ \pm 5.1^\circ$. This result supersedes the previous claim of $\lambda = 62^\circ \pm 25^\circ$ by N08, which was due to lower precision and poor statistics of the previous datasets. Thus we conclude that the HD 17156 is not strongly misaligned, and as such it joins the majority of other systems for which the RM effect has been detected (Fabrycky & Winn 2009 and references therein). If the projected spin-orbit angle is representative of the true spin-orbit angle, then the orbital tilt of HD 17156b is not so different from the orbital tilt of the Jupiter relative to the equatorial plane of the Sun.

The other TEPs for which RM observations have been reported include HAT-P-2b and XO-3b. Interestingly the outcomes of the measurements of the two systems were quite different; HAT-P-2b is also well-aligned (Winn et al. 2007b; Loeillet et al. 2008) while XO-3b has a significant spin-orbit misalignment (Hébrard et al. 2008; Winn et al. 2009b). The existence of at least some highly-inclined planets would support the notion that some TEPs have migrated through planet-planet scattering or the Kozai effect and tidal friction. However, with just three samples one cannot draw robust conclusions (see e.g. Fabrycky & Winn 2009). Further observations of the RM effect for TEPs are desired. Recently the highly eccentric, long period planet HD 80606b has been added to the list of TEPs. Observations of the RM effect for that system were presented by Moutou et al. (2009), but because of their limited time coverage a robust determination of λ is not yet possible. It will be very interesting to see the rest of the RM anomaly filled in with future observations.

We acknowledge invaluable support of our observations by Akito Tajitsu, a support scientist for the Subaru HDS. This paper is based on data collected at Subaru Telescope, which is operated by the National Astronomical Observatory of Japan. The data analysis was in part carried out on common use data analysis computer system at the Astronomy Data Center, ADC, of the National Astronomical Observatory of Japan. N.N. is supported by a Japan Society for Promotion of Science (JSPS) Fellowship for Research (PD: 20-8141). This work was

partly supported by World Premier International Research Center Initiative (WPI Initiative), MEXT, Japan. We appreciate a careful reading and quick comments by the referee, William Cochran. Finally, we wish to acknowledge the very significant cultural role and reverence that the summit of Mauna Kea has always had within the indigenous Hawaiian community.

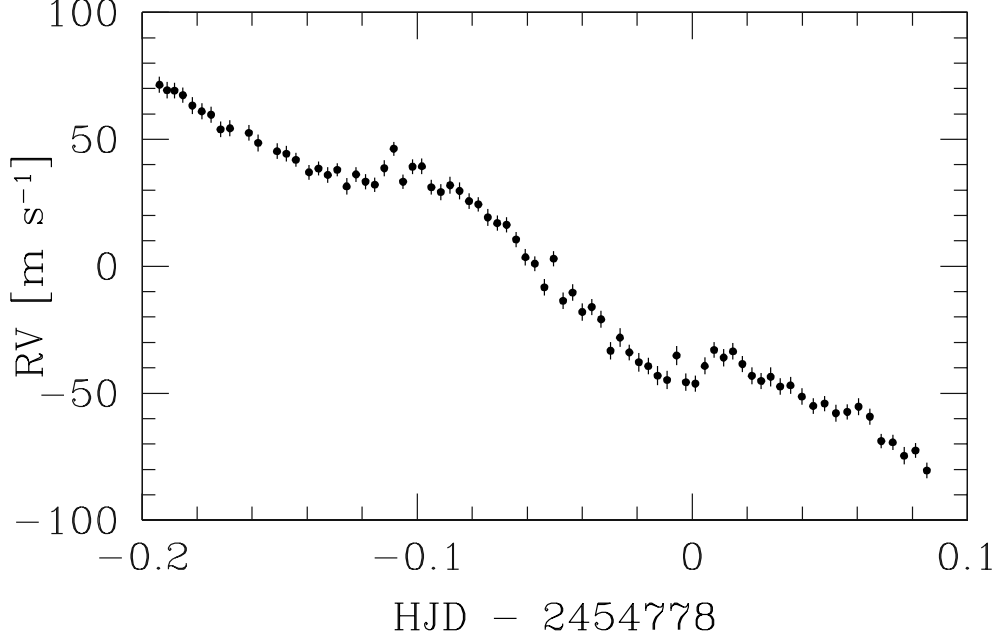


Fig. 1. Radial velocities taken with the Subaru HDS. The values and errors are presented in table 1.

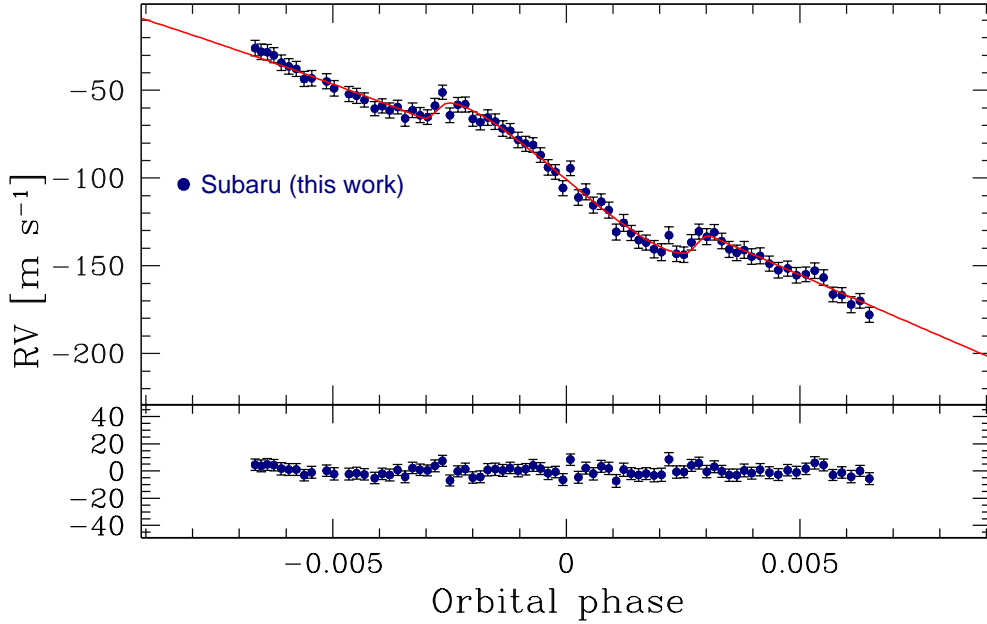


Fig. 2. The upper panel: Radial velocities and the best-fit curve of HD 17156 as a function of orbital phase. Only Subaru and Keck datasets are used. The lower panel: Residuals from the best-fit curve.

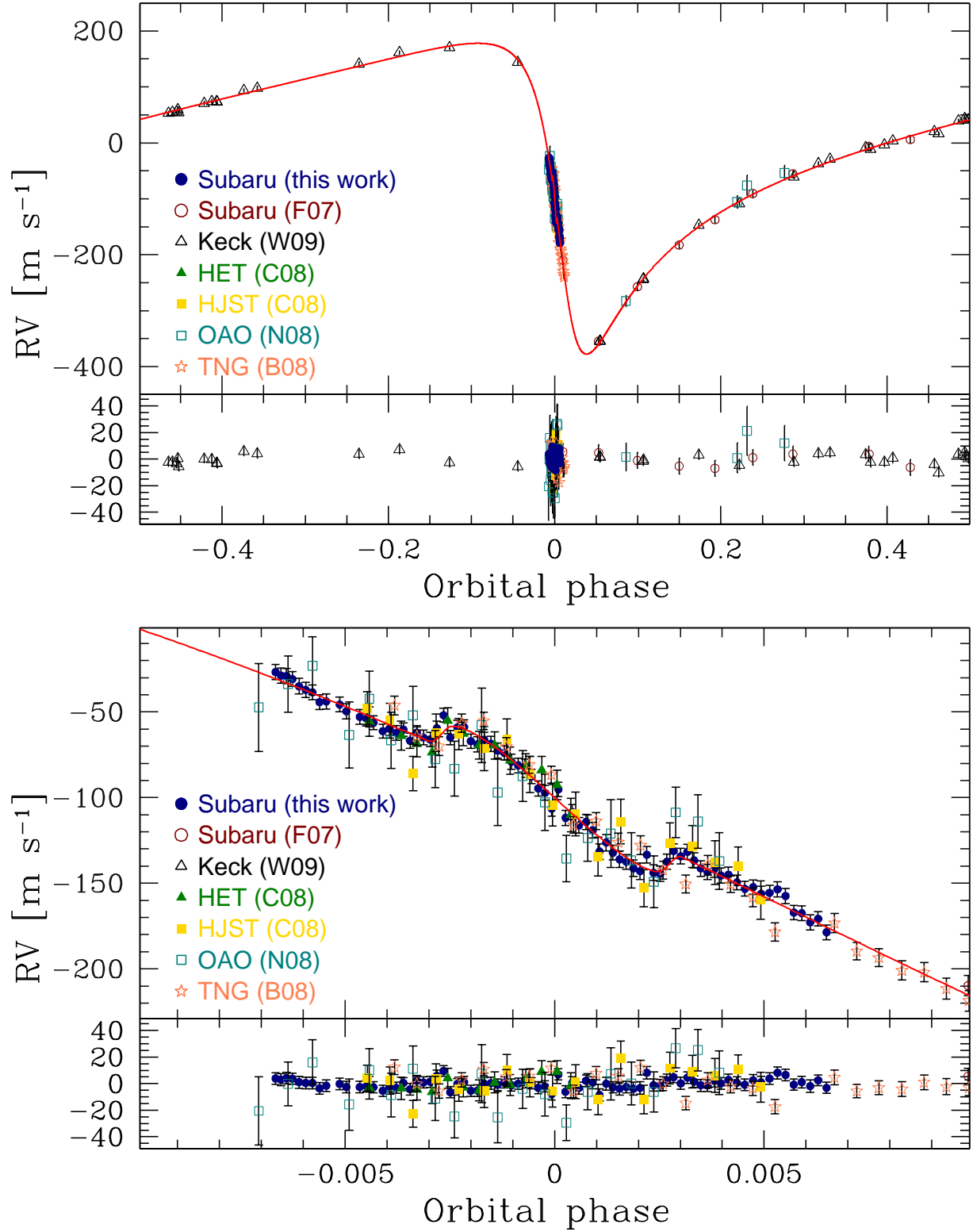


Fig. 3. The upper panels: All published radial velocities and the best-fit curve of HD 17156 as a function of orbital phase. The upper figure shows the entire orbit and the lower figure does the zoom of transit phase. The lower panels: Residuals from the best-fit curve.

Table 1. Radial velocities obtained with the Subaru/HDS.

Time [HJD]	Value [m s ⁻¹]	Error [m s ⁻¹]
2454777.80631	71.48	3.15
2454777.80904	69.36	3.26
2454777.81176	69.19	3.15
2454777.81483	67.40	3.06
2454777.81825	63.25	3.34
2454777.82166	61.08	3.15
2454777.82508	59.66	3.13
2454777.82850	53.92	3.10
2454777.83193	54.38	3.16
2454777.83877	52.56	3.12
2454777.84219	48.59	3.33
2454777.84903	45.32	3.07
2454777.85245	44.35	3.13
2454777.85587	41.94	2.81
2454777.86066	37.00	2.87
2454777.86409	38.47	2.73
2454777.86751	35.98	3.04
2454777.87093	37.97	2.59
2454777.87435	31.49	3.26
2454777.87778	36.16	2.88
2454777.88120	33.32	3.05
2454777.88461	32.15	2.82
2454777.88803	38.62	3.14
2454777.89145	46.30	2.74
2454777.89487	33.32	2.88
2454777.89829	39.22	2.85
2454777.90171	39.40	3.10
2454777.90514	31.14	2.88
2454777.90856	29.22	3.20
2454777.91198	31.93	3.30
2454777.91540	29.64	3.33
2454777.91882	25.67	3.11
2454777.92224	24.40	2.81
2454777.92566	19.20	3.32
2454777.92909	17.00	3.01

Table 1. (Continued.)

2454777.93251	16.33	3.02
2454777.93594	10.53	3.02
2454777.93936	3.58	3.31
2454777.94278	1.02	2.93
2454777.94621	-8.27	3.19
2454777.94962	3.00	2.98
2454777.95304	-13.59	3.21
2454777.95647	-10.38	3.28
2454777.96002	-18.02	3.43
2454777.96345	-16.04	3.15
2454777.96687	-20.84	3.32
2454777.97029	-33.28	3.48
2454777.97371	-28.10	3.72
2454777.97714	-33.93	3.10
2454777.98057	-37.80	3.73
2454777.98399	-39.30	3.19
2454777.98743	-43.08	3.79
2454777.99085	-44.78	3.67
2454777.99428	-35.16	3.71
2454777.99770	-45.68	3.41
2454778.00112	-46.25	3.19
2454778.00454	-39.24	3.35
2454778.00796	-32.99	3.06
2454778.01139	-36.00	3.40
2454778.01481	-33.47	3.20
2454778.01823	-38.50	3.23
2454778.02165	-43.15	3.41
2454778.02508	-45.17	3.21
2454778.02851	-43.56	3.72
2454778.03194	-47.37	3.24
2454778.03570	-46.86	3.35
2454778.03983	-51.32	3.22
2454778.04396	-55.03	3.15
2454778.04809	-54.08	3.04
2454778.05222	-57.89	3.31
2454778.05635	-57.39	3.01
2454778.06048	-55.33	3.39

Table 1. (Continued.)

2454778.06461	-59.25	3.23
2454778.06874	-68.85	2.81
2454778.07288	-69.28	3.00
2454778.07701	-74.63	3.42
2454778.08114	-72.57	2.90
2454778.08527	-80.46	3.12

Table 2. Adopted stellar and planetary parameters.

Parameter	Value	Source
$M_s [M_\odot]$	1.24	B08
$R_s [R_\odot]$	1.44	B08
R_p/R_s	0.0727	B08
a [AU]	0.1614	B08
u_1	0.39	Claret (2004)
u_2	0.37	Claret (2004)
T_c [HJD]	2454777.94761	Winn et al. in prep.
P [days]	21.2165298	Winn et al. in prep.

Table 3. Fitted values and uncertainties of the free parameters.

Parameter	Subaru and Keck		all datasets	
	Value	Uncertainty	Value	Uncertainty
K [m s ⁻¹]	275.99	±1.27	277.77	±1.19
e	0.6801	±0.0019	0.6835	±0.0017
ω [°]	121.62	±0.42	121.73	±0.41
i [°] ^a	87.21	±0.31	86.95	±0.27
$V \sin I_s$ [km s ⁻¹] ^a	4.18	±0.31	4.07	±0.28
λ [°]	10.0	±5.1	0.8	±4.3
v_1 [m s ⁻¹]	97.46	±1.57	98.23	±1.51
v_2 [m s ⁻¹]	92.89	±2.10	93.12	±2.09
v_3 [m s ⁻¹]	-0.11	±0.64	-0.20	±0.64
v_4 [m s ⁻¹]			74.21	±2.71
v_5 [m s ⁻¹]			-7850.55	±3.01
v_6 [m s ⁻¹]			142.34	±3.29
v_7 [m s ⁻¹]			146.68	±1.89

$v_1 \sim v_7$ are offset velocities for respective datasets (see Section 3).

^a: Systematic errors are not included in the uncertainties (see Section 4.2).

References

- Barbieri, M., et al. 2007, *A&A*, 476, L13
- Barbieri, M., et al. 2008, ArXiv e-prints (B08)
- Barker, A. J. & Ogilvie, G. I. 2009, ArXiv e-prints
- Butler, R. P., Marcy, G. W., Williams, E., McCarthy, C., Dosanji, P., & Vogt, S. S. 1996, *PASP*, 108, 500
- Chatterjee, S., Ford, E. B., Matsumura, S., & Rasio, F. A. 2008, *ApJ*, 686, 580
- Claret, A. 2004, *A&A*, 428, 1001
- Cochran, W. D., Redfield, S., Endl, M., & Cochran, A. L. 2008, *ApJL*, 683, L59 (C08)
- Fabrycky, D. C. & Tremaine, S. 2007, *ApJ*, 669, 1298
- Fabrycky, D. C. & Winn, J. N. 2009, ArXiv e-prints
- Fischer, D. A., et al. 2007, *ApJ*, 669, 1336 (F07)
- Gaudi, B. S. & Winn, J. N. 2007, *ApJ*, 655, 550
- Giménez, A. 2006, *ApJ*, 650, 408
- Hébrard, G., et al. 2008, *A&A*, 488, 763
- Holman, M. J., et al. 2006, *ApJ*, 652, 1715
- Ida, S. & Lin, D. N. C. 2004, *ApJ*, 616, 567
- Kurucz, R. L., Furenlid, I., Brault, J., & Testerman, L. 1984, in *Solar flux atlas from 296 to 1300 nm*, ed. R. L. Kurucz, I. Furenlid, J. Brault, & L. Testerman
- Lin, D. N. C., Bodenheimer, P., & Richardson, D. C. 1996, *Nature*, 380, 606
- Lin, D. N. C. & Papaloizou, J. 1985, in *Protostars and Planets II*, ed. D. C. Black & M. S. Matthews, 981–1072
- Loeillet, B., et al. 2008, *A&A*, 481, 529
- Marzari, F. & Weidenschilling, S. J. 2002, *Icarus*, 156, 570
- McLaughlin, D. B. 1924, *ApJ*, 60, 22
- Moutou, C., et al. 2009, ArXiv e-prints
- Nagasawa, M., Ida, S., & Bessho, T. 2008, *ApJ*, 678, 498
- Narita, N., et al. 2007, *PASJ*, 59, 763
- Narita, N., Sato, B., Ohshima, O., & Winn, J. N. 2008, *PASJ*, 60, L1+ (N08)
- Noguchi, K., et al. 2002, *PASJ*, 54, 855
- Ohta, Y., Taruya, A., & Suto, Y. 2005, *ApJ*, 622, 1118
- Pont, F., Zucker, S., & Queloz, D. 2006, *MNRAS*, 373, 231
- Press, W. H., Teukolsky, S. A., Vetterling, W. T., & Flannery, B. P. 1992, *Numerical recipes in C. The art of scientific computing* (Cambridge: University Press, —c1992, 2nd ed.)
- Rasio, F. A. & Ford, E. B. 1996, *Science*, 274, 954
- Rossiter, R. A. 1924, *ApJ*, 60, 15
- Sato, B., Kambe, E., Takeda, Y., Izumiura, H., & Ando, H. 2002, *PASJ*, 54, 873
- Takeda, G. & Rasio, F. A. 2005, *ApJ*, 627, 1001
- Winn, J. N., et al. 2005, *ApJ*, 631, 1215
- Winn, J. N., Holman, M. J., & Fuentes, C. I. 2007a, *AJ*, 133, 11
- Winn, J. N., et al. 2007b, *ApJL*, 665, L167

Winn, J. N., et al. 2009a, ApJ, 693, 794 (W09)

Winn, J. N., et al. 2009b, ArXiv e-prints

Wu, Y. & Murray, N. W. 2003, ApJ, 589, 605

Wu, Y., Murray, N. W., & Ramsahai, J. M. 2007, ApJ, 670, 820